

DESIGN OPTIMIZATION OF HELICOPTER BLADE USING CLASS SHAPE FUNCTION BASED GEOMETRY REPRESENTATION

Attaphon Ariyarat*, Masahiko Sugiura**, Yasutada Tanabe**, and Masahiro Kanazaki*

*Department of Aerospace Engineering, Graduate School of System Design, Tokyo Metropolitan University

**Institute of Aeronautical Technology, Japan Aerospace Exploration Agency

Keywords: Helicopter Blade Design, Shape Optimization, Multi-objective Optimization, Blade Element Momentum Theory

Abstract

In this paper, a twist distribution of the helicopter blade is optimized to maximize the helicopter efficiency and the influence of the required power is investigated. A multi-objective optimization problem was set to search optimal designs for hovering and forward flight condition. The efficiency of helicopter rotor blade for hovering can be measured by a figure of merit and for a forward flight can be measured by the ratio between Thrust (C_T) and a summation value of in-plane H force (C_H) and total torque (C_Q) divided by the advance ratio (μ). Blade element momentum theory is deployed to evaluate the design for forward flight and hovering conditions. The twist distribution of helicopter blade is controlled by the class shape function transformation parameterization. The Non-dominated Sorting Genetic Algorithm with multi-modal distribution crossover method was used to solve multi-objective optimization problems. From results of optimization problem found that the twist has an effect of the change in drag force that acts on the blade structure on the figure of merit.

1 Introduction

The main helicopter rotary wing generates the main lifting force for a helicopter and is essential to a helicopter's performance. A helicopter blade design is a complicated problem because a helicopter always flies with a different speed [1,2]. A multi-objective

optimization method is used to find optimal designs with different flying speed.

The class shape transformation (CST) [3] parameterization was used to control a helicopter blade shape because it can be generated many kinds of shape by only one shape function. From the previous studies, twist distributions are sensitive to a helicopter blade performance. Consequently, twist distribution was chosen to control a helicopter blade shape in this study. In addition, a twist distribution close to a blade tip has more effect on helicopter blade performance than twist distribution close to a blade root. From this reason, twist distributions represented by CST, was applied for generating a blade shape close to a blade tip. Twist distribution close to a blade tip is shown in Fig. 1

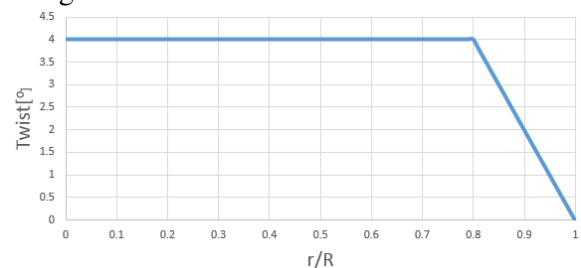


Fig.1 Twist distribution.

One of the most popular of multi-objective optimization methods is Non-dominated Sorting Genetic Algorithm (NSGA-II) [4] was selected as a multi-objective optimization method. However, the main operators of GA are the selection, crossover and mutation operator. In particular, the crossover operator is effective for increasing an efficiency of an optimization process. The multi-modal

distribution crossover (MMDX) [5] method was selected as a crossover method in this optimization process because this crossover method can maintain higher diversity and has fast divergence rate. That it can reduce the computation time for an optimization process.

2 Blade Design Method

2.1 CST

The CST [3] is one kind of a parameterization method for constructing the shape that is used for the global design exploration. The advantage of the CST is a simplicity of creating the shape by controlling only the weight factors. Kulfan and Bussoletti propose the CST by representing a two-dimensional geometry which consists of a product from a class function, $C(x/c)$, a shape function, $S(x/c)$, and a term that characterizes the trailing edge thickness (Δz_{te}) by following expressions:

$$\frac{y}{c} \equiv C\left(\frac{x}{c}\right)S\left(\frac{x}{c}\right) + \frac{x}{c} \frac{\Delta z_{te}}{c} \quad (1)$$

where $C(x/c)$ is given by generic form:

$$C\left(\frac{x}{c}\right) \equiv \left(\frac{x}{c}\right)^{N_1} \left[1 - \frac{x}{c}\right]^{N_2} \quad \text{for } 0 \leq \frac{x}{c} \leq 1 \quad (2)$$

The shape function $S(x/c)$ is defined on the basis of the Bernstein binomials by the weight factor b_i as follows:

$$S\left(\frac{x}{c}\right) = \sum_{i=0}^n \left[b_i \cdot K_{i,n} \left(\frac{x}{c}\right)^i \cdot \left(1 - \frac{x}{c}\right)^{n-i} \right] \quad (3)$$

where $K_{i,n}$ is given as

$$K_{i,n} = \frac{n!}{i!(n-i)!} \quad (4)$$

The definition of CST is shown in Fig. 2.

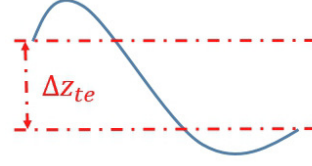


Fig. 2 Definition of CST.

2.2 NSGA-II

Genetic algorithm (GA) is a stochastic search method using the genetic operators such as the selection, crossover and mutation. Figure 3 shows the algorithms of simple GA. In this work, the NSGA-II [4] was selected to search the minimum mass and stress of structure. NSGA-II is widely employed to solve multi-objective problem. NSGA-II is characterized by nondominated points and crowding distance sorting. The individuals of the next generation are selected by elitism. The new generation is filled by each front sequentially until the population size exceeds the current population size (shown in Fig. 4). In this work, the MMDX crossover [5] (shown in Fig. 5) and the simple mutation are also applied.

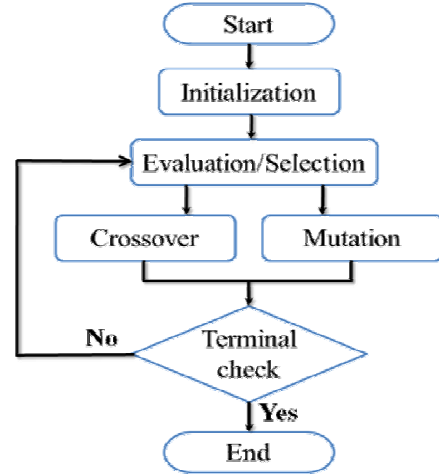


Fig. 3 Algorithm of GA.

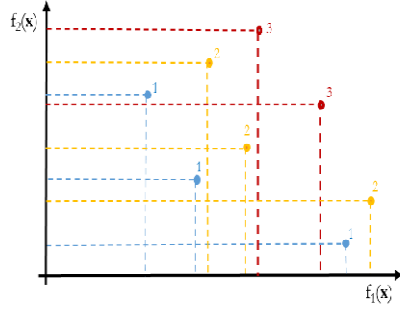


Fig. 4 Ranking by NSGA-II (Minimization f_1 and f_2)

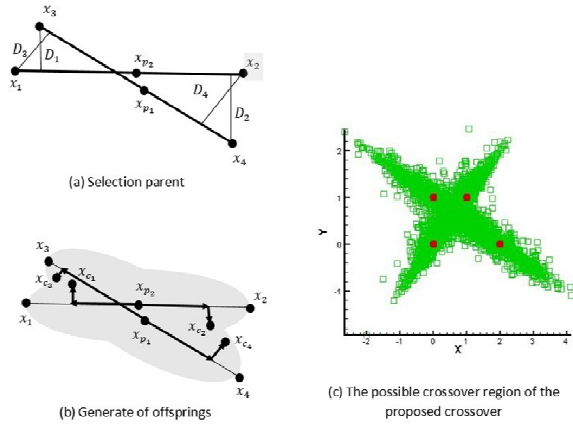


Fig. 5 Schematic illustration and possible crossover region of MMDX crossover.

3 Evaluation of Helicopter Rotor Blade

3.1 Hovering

The parallel coordinate plot (PCP) [5] is one of the statistical visualization techniques for displaying high-dimensional data at a glance in a two-dimensional graph. To create the PCP, the attribute values in the design problem must be normalized to allow comparison in the same axis. After the normalization, the axes are arranged in a parallel line. Generally, the distances between one line and the next are equivalent. In this study, the normalization value p_i from the design variable dv is given below.

$$p_i = \frac{dv_i - dv \min_i}{dv \max_i - dv \min_i} \quad (5)$$

where $dv \min_i$ represents the lower bound of the i^{th} design variable and $dv \max_i$ denotes the upper bound of the i^{th} design variable.

3 Evaluation of Helicopter Rotor Blade

3.1 Hovering

In this work, we use the theory of blade element theory (BEMT) [6,7] to evaluate the helicopter rotor blade. In the BEMT, BEMT calculates the forces on the blade, which is then used to compute the performance of blade. The blade is divided into a number of independent section and the assumption of section with two-dimensional air-foil for calculating the force in each section is assumed. The process of BEMT begin with using the momentum theory to find the inflow distribution (λ) for hovering by following equation:

$$\lambda = \frac{\sigma a}{16} \left[\sqrt{1 + \frac{32}{\sigma a} \theta r} - 1 \right] \quad (6)$$

where σ is solidity which can be obtained from:

$$\sigma = \frac{Nc}{\pi R} \quad (7)$$

N is the number of blades, c is the chord length, R is a rotor blade radius, θ is a pitch angle, and a is a blade section two-dimensional lift-curve slope.

Next the section inflow angle is calculated by:

$$\Phi = \tan^{-1} \left(\frac{\lambda}{\Omega r} \right) \quad (8)$$

where Ω is an angular velocity and r is a blade radial coordinate.

An angle of attack, an inflow angle and a pitch angle of each element is described in Fig.4. From the Fig.4, the angle of attack can be calculated from: $\alpha = \theta - \Phi$. A drag coefficient (C_d) and a lift coefficient (C_l) are computed from the angle of attack or from using data in the airfoil profile table.

The section forces in terms of the lift and the drag coefficients yields:

$$L = \frac{1}{2} \rho U^2 c c_l \quad (9)$$

$$D = \frac{1}{2} \rho U^2 c c_d \quad (10)$$

where ρ is an air density and U is a resultant velocity magnitude. The explanation of U is also shown in Fig. 4 and U can be computed from:

$$U = \sqrt{u_T^2 + u_p^2} \quad (11)$$

Resolving the aerodynamic forces normal (F_z) and (F_x), which are parallel to the disk plane gives:

$$F_z = L \cos \Phi - D \sin \Phi \quad (12)$$

$$F_x = L \sin \Phi + D \cos \Phi \quad (13)$$

The elemental thrust, a torque, and a power on the rotor are:

$$dT = NF_z dr \quad (14)$$

$$dQ = NF_x r dr \quad (15)$$

$$dP = \Omega dQ = NF_x \Omega dr \quad (16)$$

where Ω is blade angular velocity. Finally, the figure of merit (FOM), which measures rotor blade performance, is defined as:

$$FOM = \frac{T \sqrt{T / 2 \rho A}}{P} \quad (17)$$

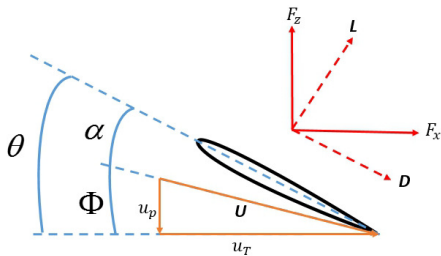


Fig. 6 Blade section aerodynamics.

3.2 Forward Flight

The BEMT [6,7] also applied to a forward flight condition. In forward flight condition, the BEMT process start with calculated the advance ratio that expressed as:

$$\mu = \frac{V}{\Omega R} \quad (18)$$

Where V is the flight velocity.

According to Fig. 7, the components u_T and u_R are defined as:

$$u_T = r + \mu \sin \psi \quad (19)$$

$$u_R = \mu \cos \psi \quad (20)$$

where ψ is azimuth position. According to Fig. 8, an inflow factor is given as:

$$\lambda = \mu \alpha_r + \lambda_i \quad (21)$$

The λ can be defined from the linear inflow variation:

$$\lambda = \lambda_0 (1 + k_x r \cos \psi) \quad (22)$$

where

$$k_x = (15\pi / 23) \tan(\chi / 2) \quad (23)$$

$$\chi = \tan^{-1} \frac{\mu}{\lambda} \quad (24)$$

and λ_0 is the mean induced velocity that given as:

$$\lambda_0 = \frac{C_T}{2\sqrt{\mu^2 + \lambda_0^2}} \quad (25)$$

The component u_p is given as:

$$u_p = \lambda + \beta \mu \cos \psi + r \frac{d\beta}{d\psi} \quad (26)$$

where β is a coning angle. In this study, β is set to 0 because a rigid rotor type is used and the flapping angle is suppressed at the blade root. The component u_T is given as:

$$u_T = r + \mu \sin \psi \quad (27)$$

For small angles the resultant velocity U can be approximated by u_T by:

$$\alpha = \theta - \Phi = \theta - \frac{u_p}{u_T} \quad (28)$$

The thrust coefficient (C_T), H-force coefficient (C_H) and Torque coefficient (C_Q) with small angles is defined as:

$$C_T = \int_0^1 \frac{1}{2} \sigma a (\theta u_T^2 - u_T u_p) dr \quad (29)$$

$$C_H = \sigma a \int_0^1 \left\{ \sin \psi \left[\frac{1}{2} (u_p u_T \theta - u_p^2) + \frac{c_d}{2a} u_T^2 \right] \right\} dr \quad (30)$$

$$C_Q = \sigma a \int_0^1 \left\{ r \left[\frac{1}{2} (u_p u_T \theta - u_p^2) + \frac{c_d}{2a} u_T^2 \right] \right\} dr \quad (31)$$

Finally, the efficiency of helicopter blade for forward flight can be measured by

$$Eff = \frac{C_T}{C_H + C_q / \mu} \quad (32)$$

The Eff value is equivalent to the effective lift per drag ratio (L/D) of the rotor in forward flight.

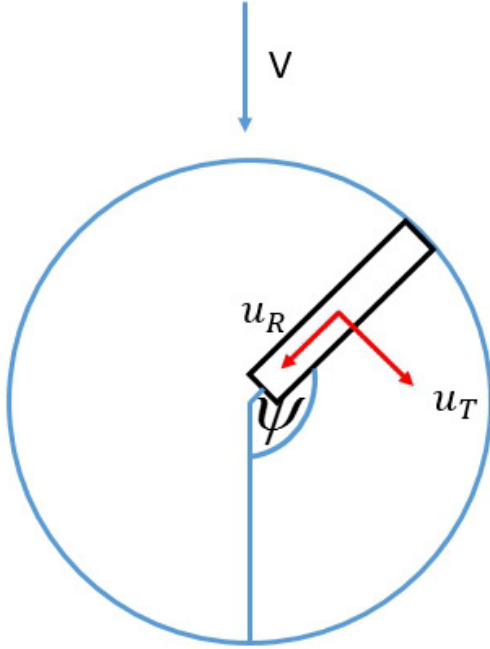


Fig. 7 Component velocities u_T and u_R .

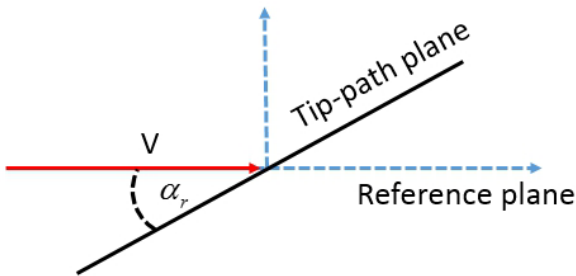


Fig. 8 Component velocities in forward flight.

4 Designing Problem

In this research, the twist angle is designed. The CST is defined in Fig 9. Three weight factor (b_i) are considered to design the distributions. The design parameters of the rotary wing geometry that are created by the CST is shown in Table 1. The conditions for calculating the helicopter performance for hovering and forward flight are shown in Table

2. The objective function for hovering is FOM and for forward flight is Eff . The optimization problem considered in this study can be written as follows:

Maximize: FOM (For hovering)

Maximize: Eff (For forward flight)

The optimization results are compared with the baseline. The rotary wing properties are shown in Table 3 and the location of a start point (L) is 0.7. In this optimization problem, the number of iteration and population are set to 100 and 100.

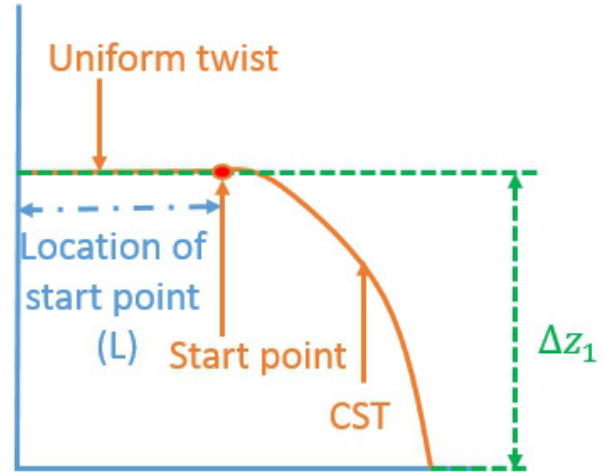


Fig. 9 Twist distributions from CST.

Table 1 Design parameters.

Design Factor		Value
b_i for twist (three parameters)	dv1-dv3	-1.0 – 1.0
Δz	dv4	0 - 10

Table 2 Calculation conditions.

C_T / σ	0.1
Rotation speed (rpm)	1041.0
Thrust target (N)	5636
Speed for forward flight (m/s)	66
Advanced ratio (μ)	0.3

Table 3 Baseline rotary wing properties.

The number of blades	0.1
Rotor radius (m)	2.0
Chord length (m)	0.121
Airfoil	NACA23012

5 Results

Figure 10 shows the history of the hypervolume, which it used to show the convergence rate of multi-objective optimization problem by measure the volume of non-dominated solution in each iteration, for finding the rotary wing optimum design. This figure can show the optimization process converges after 25th iteration.

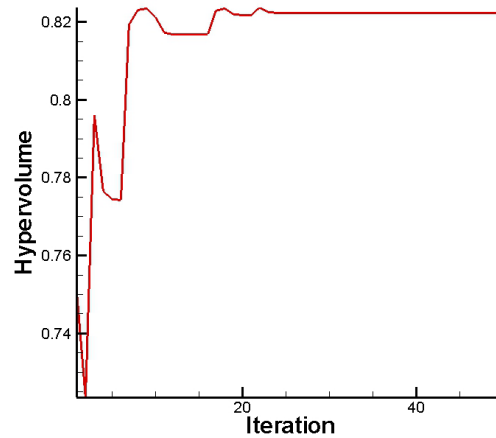


Fig. 10 Hypervolume.

The non-dominated solution of this optimization problem is shown in Fig.11. According to this figure, optimal solutions of hovering case have the range between $FOM = 0.78$ to 0.828 and optimal solutions of forward flight case have the range between $EFF = 5.8$ to 6.04 . Figure 12 shows the optimal shape that can be obtained the highest FOM , the highest Eff and the median from non-dominated solution in Fig.11.

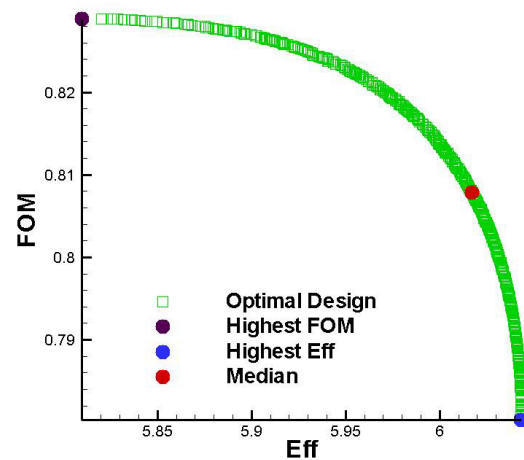


Fig. 11 Resulting non-dominated solutions.

Figure 13 (a) shows the optimal shapes that obtain the performance from Fig. 11. Figure 13 (b) shows the optimal shape only the twist distribution at the design space ($0.7 \leq r/R \leq 1.0$), which the shape at design spaces are created by CST. According to Fig. 12 and 13, the results show the Δz parameter ($dv4$) will affect the performance of hovering and forward flight problems. If the Δz has a high value, the helicopter blade will have higher performance for hovering problem. On the other hand, if Δz has low value the helicopter blade will have higher performance for forward flight condition. Figure 12 and 13 shows a shape that has Δz equal to 0.39 can be obtained the maximum Eff and a shape that has Δz equal to 5.85 can be obtained the maximum FOM . The PCP plot shows a relationship between each design variable and target objectives is shown in Fig.14.

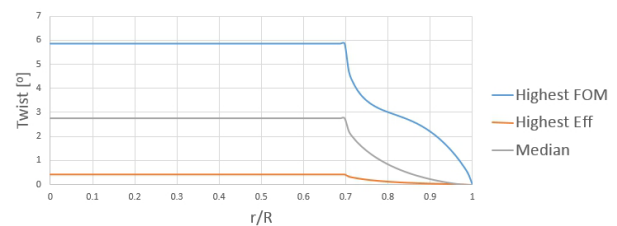


Fig. 12 The highest FOM , highest Eff and median of optimal blade shape.

DESIGN OPTIMIZATION OF HELICOPTER BLADE USING CLASS SHAPE FUNCTION BASED GEOMETRY REPRESENTATION

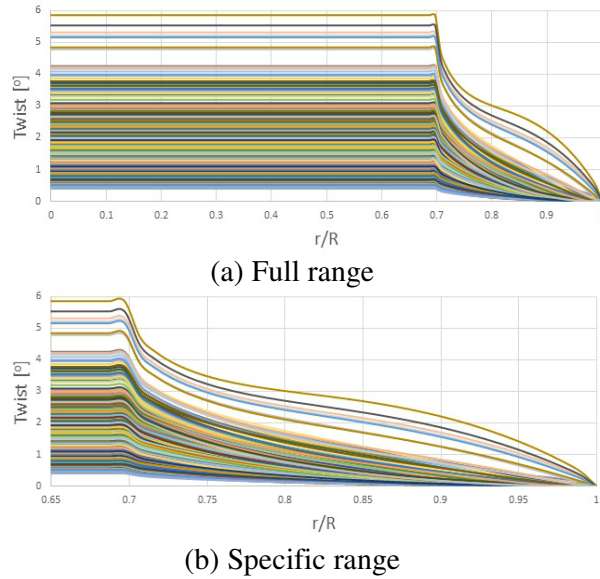


Fig. 13 Optimal blades geometry.

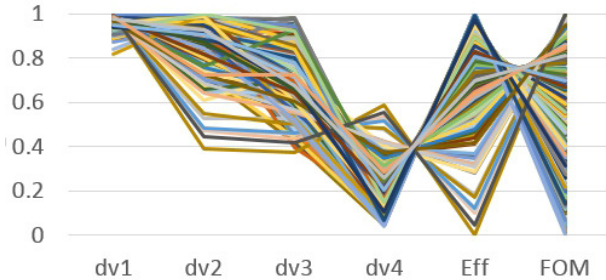


Fig. 14 The PCP of the non-dominated solution.

5 Conclusion

This paper finds the multi-objective optimal design of helicopter blade using CST representation method. The objective of this research is to find the helicopter blade that has the highest performance in hovering and forward flight condition. The original CST was used to construct helicopter rotor blade by controlling the twist distributions. NSGA-II with MMDX crossover method was deployed to find the helicopter rotor blade. The BEM method was applied to calculate the helicopter blade performance.

The results of multi-objective optimization show the twist distribution has effect to the performance of helicopter blade performance and the optimal performance for hovering condition has in the range between $FOM = 0.78$ to 0.828 and the optimal performance for forward flight condition has in

the range between $Eff = 5.8$ to 6.4 . Results of optimal shape also shown the twist angle is a trade-off to the performance of hovering and forward flight condition. A blade shape that has small twist angle has better performance for forward flight condition and a blade shape that has high twist angle has better performance for hovering.

References

- [1] Sugiura, M., Tanabe, Y., Sugawara, H., Takeda, S. and Kanazaki, M. "Computationally Efficient and High Fidelity Optimization," 40th ERF, September 2-5, 2014.
- [2] Takeda, S., Tanabe, Y., Sugawara, H. Kanazaki, M. and Tsuijii, T. "Optimization of the blade tip chord length and twist distribution in hover," 8th Australian Pacific Vertiflite Conference on Helicopter Technologies and 3rd Asian Australian Rotorcraft Forum, Melbourne, Australia, December 18-19, 2014.
- [3] Kulfan, Brenda M. "Universal parametric geometry representation method." *Journal of Aircraft* 45.1 (2008): 142-158.
- [4] K. Deb, et al., A Fast and Elitist Multiobjective Genetic Algorithm: NSGA-II. *IEEE Transactions on Evolutionary Computation*, 6(2) (2002), 182-197.
- [5] Ariyarat, A., and Kanazaki, M. "Multi-modal distribution crossover method based on two crossingsegments bounded by selected parents applied to multi-objective design optimization." *Journal of Mechanical Science and Technology* 29.4 (2015): 1443-1448.
- [6] Johnson, Wayne. *Rotorcraft Aeromechanics*. Vol. 36. Cambridge University Press, 2013.
- [7] Leishman, J. Gordon. *Principles of Helicopter Aerodynamics with CD Extra*. Cambridge university press, 2006.

Copyright Statement

The authors confirm that they, and/or their company or organization, hold copyright on all of the original material included in this paper. The authors also confirm that they have obtained permission, from the copyright holder of any third party material included in this paper, to publish it as part of their paper. The authors confirm that they give permission, or have obtained permission from the copyright holder of this paper, for the publication and distribution of this paper as part of the ICAS proceedings or as individual off-prints from the proceedings.